

Portland State University

**PDXScholar**

---

REU Final Reports

Research Experiences for Undergraduates  
(REU) on Computational Modeling Serving the  
City

---

8-24-2019

# Modeling the Defects That Exists in Crystalline Structures

Kiet A. Tran

*Portland State University*

Follow this and additional works at: [https://pdxscholar.library.pdx.edu/reu\\_reports](https://pdxscholar.library.pdx.edu/reu_reports)



Part of the [Other Mathematics Commons](#), and the [Other Physical Sciences and Mathematics Commons](#)

Let us know how access to this document benefits you.

---

## Citation Details

Tran, Kiet A., "Modeling the Defects That Exists in Crystalline Structures" (2019). *REU Final Reports*. 13.  
[https://pdxscholar.library.pdx.edu/reu\\_reports/13](https://pdxscholar.library.pdx.edu/reu_reports/13)

This Report is brought to you for free and open access. It has been accepted for inclusion in REU Final Reports by an authorized administrator of PDXScholar. Please contact us if we can make this document more accessible:  
[pdxscholar@pdx.edu](mailto:pdxscholar@pdx.edu).

# Modeling the Defects that exists in Crystalline Structures

Kiet Tran, Dow Drake, Jay Gopalakrishnan, Saurabh Puri  
trankiet@pdx.edu  
Portland State University

August 2019

# 1 Abstract

This paper focuses on modeling defects in crystalline materials in one-dimension using field dislocation mechanics (FDM). Predicting plastic deformation in crystalline materials on a microscopic scale allows for the understanding of the mechanical behavior of micron-sized components. Following Das et al (2013), a one dimensional reduction of the FDM model is implemented using Discontinuous Galerkin method and the results are compared with those obtained from the finite difference implementation. Test cases with different initial conditions on the position and distribution of screw dislocations are considered.

Keywords: Field Dislocation Mechanics, Plasticity, Plastic Deformation

## 2 Introduction

This project is focused on modeling defects in crystalline materials. In crystalline materials, atoms are arranged in an ordered pattern that repeats itself in three-dimensions. Figure 1 shows the arrangement of atoms in a hexagonal close-packed crystal structure.

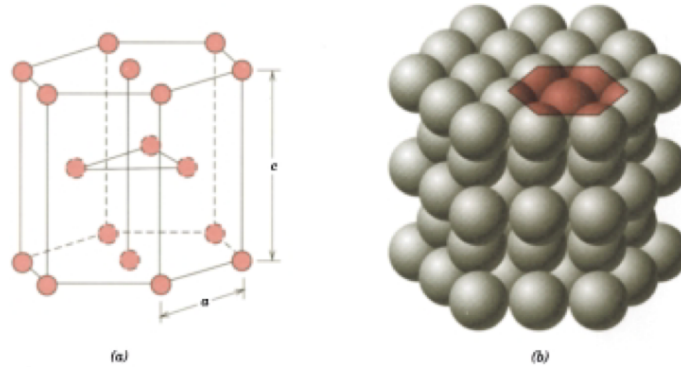


Figure 1: Hexagonal close-packed crystal structure (Callister, 2001)

Over the last few decades, crystalline materials have found increasing use in technology, energy, and other sectors. The properties of crystalline materials significantly depend on the arrangement of atoms as well as defects in this arrangement. In order to design novel crystalline materials with desired properties, it is very important to understand the nucleation and evolution of defects in the ordered structure. Some of the defects observed in crystals are voids (point defect), dislocations (line defect), and grain boundaries. One of the interesting properties of these materials is their ability to deform permanently on applying stress. This characteristic is called plasticity and is caused by the motion of line defects called dislocations. Dislocations are line defects in the regular arrangement of atoms. There are two types of dislocations that exist in the materials, edge and screw dislocation. In an edge dislocation, an extra half plane of atoms is present in the crystal, as shown in Figure 2. The lattice of atoms distorts close to the dislocation; however, the crystal structure is perfect away from the dislocation (Callister, 2001). When stress is applied, this extra half plane of atoms moves and leaves a step on the surface as shown in Figure 4. The edge of the extra half plane terminates in the crystal and is called a dislocation line. In an edge dislocation, dislocation line is perpendicular to the direction of motion of a dislocation (Figure 4). The direction and magnitude of motion of a dislocation is represented by Burgers vector. Thus, in an edge dislocation, Burgers vector is perpendicular to the dislocation line. A screw dislocation is characterized by the relative shift in the upper and lower portion of the crystal, as shown in Figure 3 (Callister, 2001). In the case of a screw dislocation, Burgers vector is parallel to the dislocation line.

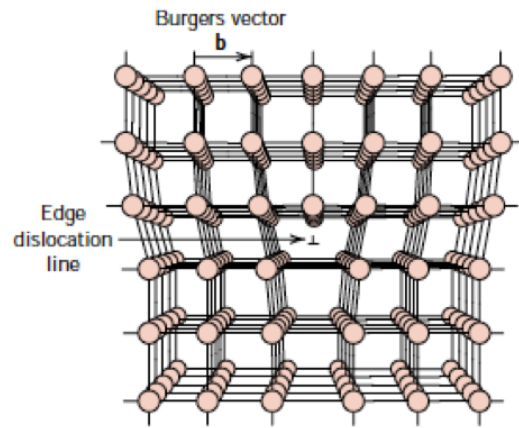


Figure 2: Edge Dislocation (Callister, 2001)

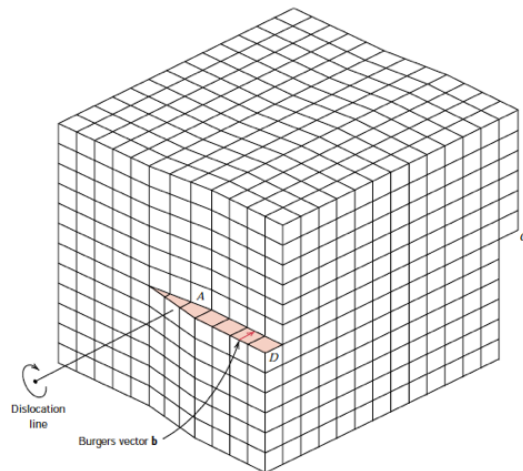


Figure 3: Screw Dislocation (Callister, 2001)

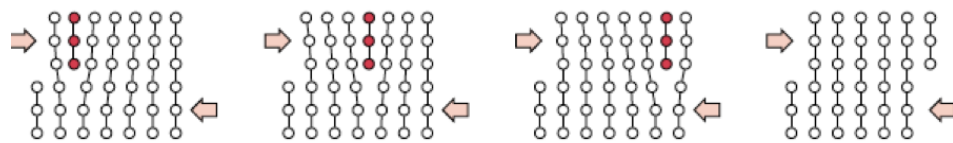


Figure 4: Motion of an edge dislocation (Callister, 2001)

In real crystals, dislocations mostly exist as mixed dislocations (edge and screw). Dislocation lines can be straight or curvilinear in three dimensions and can be observed using advanced electron microscopes. Transmission electron microscope was used to observe the dislocation lines in a sample shown in Figure 5 (Dimiduk et al, 2006).

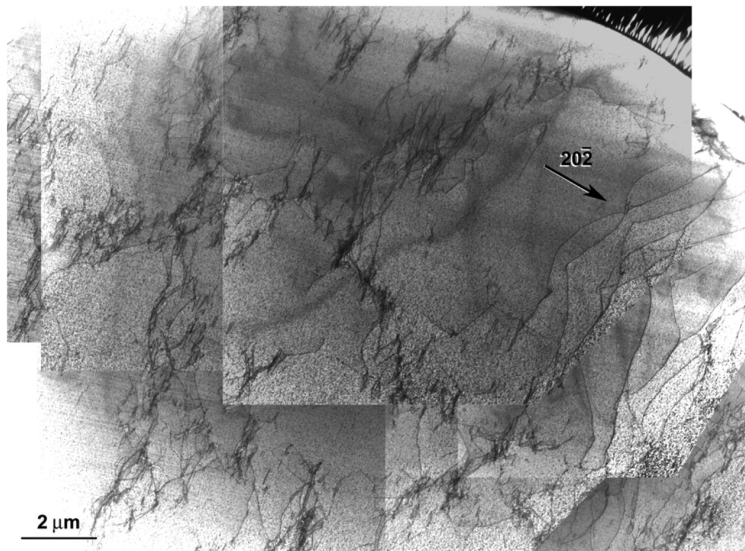


Figure 5: Dislocations in a sample (Dimiduk et al., 2006)

Dislocations move in a crystal on a preferred plane and in a preferred direction. The preferred plane is called a slip plane and the direction is called a slip direction. A slip plane and a slip direction together form a slip system. A Face Centered Cubic structure has 12 slip systems.

A thorough understanding of the nucleation and evolution of dislocations is required to predict plastic deformation mechanisms in crystalline machine components in current operating conditions as well as to design superior materials that could sustain severe thermomechanical conditions. Theories and computational frameworks that could model dislocation evolution and quantitatively predict their highly nonlinear interactions with obstacles remain elusive. The reliable atomistic methods are computationally intensive. The highly efficient macroscopic elasto-plastic constitutive models are not able to predict few of the experimental observations. One of such observations is the size effect shown in Figure 6 (Uchic et al., 2004). Uchic et al. (2004) performed uniaxial compression tests with pillar shaped specimens of Ni. The diameter of specimens varied from 5 microns to 40 microns. Some of the key observations were, (i) smaller samples show a harder response, (ii) smaller samples show different stress-strain response for the same size, and (iii) scatter in the response decreases with the increase in size of the specimen. Thus, macroscopic elastoplastic models cannot

be used for predicting the mechanical behavior of micron-sized components.

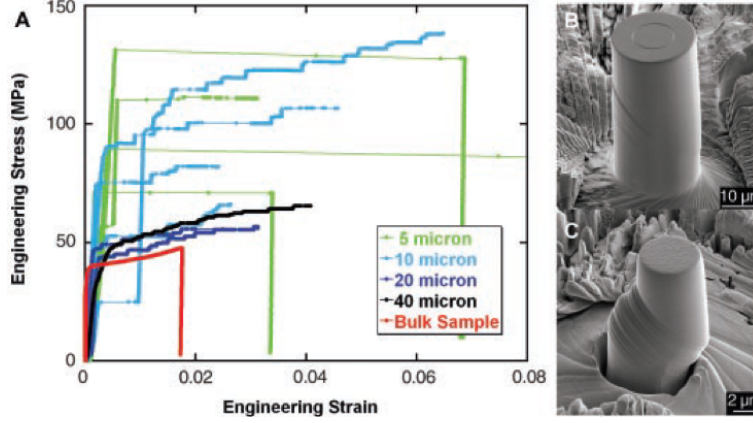


Figure 6: (A) Stress-strain response of Ni pillars; (B) Scanning Electron Microscope (SEM) image of 20 micron diameter sample; (C) SEM image of 5 micron diameter sample (Uchic et al., 2004).

In this project, a field model of dislocation mechanics (Acharya 2010), which has the potential to overcome these issues, is used. The field dislocation mechanics (FDM) model can predict the evolution of an arbitrary configuration of dislocations and the related stress field and distortion. Focus is to develop an efficient and reliable implementation of FDM using advanced numerical methods, such that the developed computational framework is able to explicitly model the fine scale phenomenon involving few dislocations. Applications of such a framework are many. One of the applications is in the design of semiconductor materials. The developed framework can be used to exploit the effect of strain field of dislocations on the electronic band structure.

A finite difference based implementation of the one-dimensional reduction of the FDM model exists (Das et al, 2013). This implementation has been able to model single dislocation as well as interaction of few dislocations. FDM model has also been used to study the interaction of dislocations in two dimensions in Zhang et al. (2015). In Zhang et al. (2015), a composite setup is considered, as shown in Figure 7. In the composite, an elastoplastic layer with linearly elastic regions on the top and bottom is considered. Dislocations are allowed to evolve in the plastic layer but no dislocation is present in the elastic layers. Dislocation evolution is calculated using the finite difference implementation of the 1d FDM equation in the plastic layer. The resulting plastic strain is used for solving the stress equilibrium equation for the whole specimen using finite element method. Thus, for every new slip plane, a one-dimensional finite difference implementation based slip layer needs to be introduced. This process gets more complicated in three dimensions. Our intent is to develop a technique that does not need such a slip layer. We plan to use advanced discontinuous Galerkin method for numerical implementation of the model. A one-dimensional

implementation of the FDM model is used in this project.

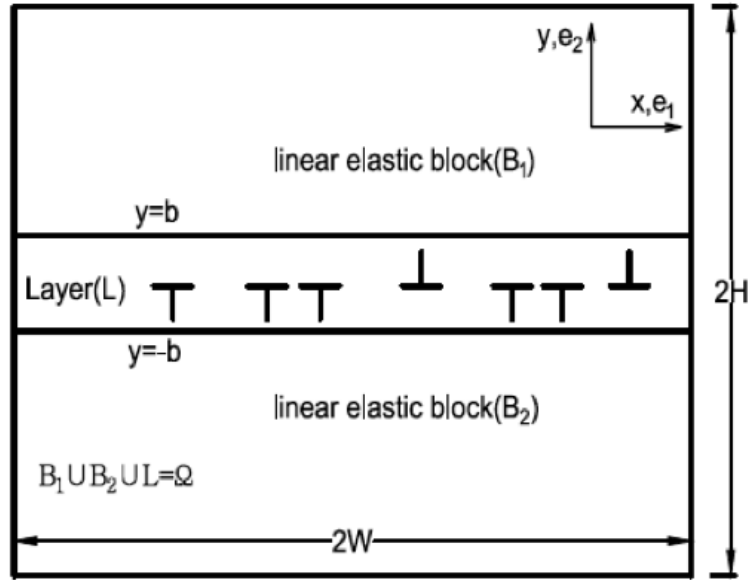


Figure 7: Composite structure used in Zhang et al. (2015)

This report is organized as follows: Field dislocation mechanics model with initial and boundary conditions is described in Section 3, nondimensionalization of equations is described in Section 4, the implementation of this model and approaches used to solving and simulating the FDM model is described in Section 5, the dislocation results for the different initial conditions when subject to load and no load is described and analyzed in Section 6, and the conclusions along with future plans is described in Section 7.



### 3 Mathematical Statement of the Dislocation Problem

Many physical problems can be represented in the form of a partial differential equation. The mechanics of dislocations, considered in this project, is also represented by a partial differential equation in the FDM model.

In this section, the three dimensional FDM model, one dimensional reduction of the model, initial and boundary conditions, problem setup and material properties are discussed.

#### Three-Dimensional Model

When examining a static model of no forces or inertia, the stress tensor  $\mathcal{T}$  is satisfied by the equation:

$$\text{div } \mathcal{T} = 0$$

Standard displacement boundary conditions are used in this model and the elastic distortion tensor  $U^e$  is defined as:

$$U^e = \text{grad}(u) - U^P$$

where  $u$  is the total displacement field and  $U^P$  is the plastic distortion tensor.

The evolution of polar dislocation density follows the conservation of Burgers vector,

$$\dot{\alpha} = -\text{curl}(\alpha \times V) \tag{1}$$

where  $\alpha \times V$  is the time derivative of the plastic deformation  $\dot{U}^P$ ,

$$\dot{U}^P = \alpha \times V. \tag{2}$$

Given the stress tensor  $\mathcal{T}$  along with some polar dislocation velocity  $V$ , it is possible to solve the system of three-dimensional equations to understand plastic deformation. We consider the case

$$V = \frac{1}{\tilde{B}} \left( \mathcal{T} + \kappa \text{curl } \alpha - \frac{\partial \eta}{\partial U^p} \right) \times \alpha \tag{3}$$

where  $\kappa$  is a material constant,  $\eta$  is an energy functional, and  $\tilde{B}$  is a material constant.

#### Reduction to a One-Dimensional Model

When reducing the model to a one-dimensional system, only one component of  $U_{12}^P$  is considered to be non-zero.

The one-dimensional system of equation becomes:

$$\dot{\alpha} + \partial_z(\alpha V) = 0 \tag{4}$$

$$\dot{\phi} + \alpha V = 0 \quad (5)$$

$$V = -\frac{1}{\bar{B}}(\mathcal{T} - \eta_\phi + \kappa \partial_z \alpha) \alpha \quad (6)$$

$$\mathcal{T} = f(\phi, t) \quad (7)$$

Here, some of the terms and variables are redefined to simplify notation, where  $z:=x_3$ ,  $\phi=U_{12}^P$ ,  $\frac{\partial \eta}{\partial U^P}=\eta_\phi$ .  $V$  represents the dislocation velocity,  $\dot{\alpha}$  is the derivative of dislocation density with respect to time,  $\dot{\phi}$  is the derivative of plastic distortion with respect to time, and  $\mathcal{T}$  is a function f of  $\phi$  and time. Along with these system of equations, the assumption of applied strain  $g(t)$  is also defined as  $u_1(x_2, t)=g(t)x_2$ , so that  $\partial_2 u_1=g(t)$ .

In this paper we consider two separate cases of stress  $f(\phi, t)$ :

Linear Stress:

$$f(\phi, t) = \frac{c}{2}(g(t) - \phi) \quad (8)$$

Cubic Stress:

$$f(\phi, t) = \frac{c}{2(\frac{\bar{\phi}}{2})^2}(g(t) - \phi - \frac{\bar{\phi}}{2})((g(t) - \phi - \frac{\bar{\phi}}{2})^2 - (\frac{\bar{\phi}}{2})^2) \quad (9)$$

Equation (9) is extended periodically outside the range  $(0, \bar{\phi}]$ .  $g(t)$  represents the applied strain. Equation (8) represents a linear stress and equation (9) represents a cubic stress.

## Initial Conditions and Boundary Conditions

The following initial conditions are used to test several different cases for  $\phi$  and  $\alpha$  with varying applied strains  $g(t)$  and with both linear and cubic shear stress  $f(\phi, t)$  cases. Neumann boundary conditions are applied for  $\alpha$  and  $\phi$ , which prescribes a flux over the outward normal on the boundary.

Single Dislocation Connecting Wells

$$\phi(z, 0) = \frac{\bar{\phi}}{2}(-1 + \tanh(z)) \quad (10)$$

$$\alpha(z, 0) = \frac{\bar{\phi}}{2}(1 - \tanh^2(z)) \quad (11)$$

Single Dislocation Between Wells

$$\phi(z, 0) = 0.015(-1 + \tanh(z)) + 0.01 \quad (12)$$

$$\alpha(z, 0) = 0.015(1 - \tanh^2(z)) \quad (13)$$

Single Dislocation Between Wells Non-Equidistant from Energy Wells

$$\phi(z, 0) = 0.015(-1 + \tanh(z)) + 0.005 \quad (14)$$

$$\alpha(z, 0) = 0.015(1 - \tanh^2(z)) \quad (15)$$

Two Dislocations of Opposite Sign Between Wells

$$\phi(z, 0) = 0.01275(1 + \tanh z) + 0.012, -\infty < z < 50 \quad (16)$$

$$\phi(z, 0) = -0.01275(1 + \tanh(z - 100)) + 0.0375, 50 \leq z < \infty \quad (17)$$

$$\alpha(z, 0) = 0.01275(1 - \tanh^2(z)), -\infty < z < 50 \quad (18)$$

$$\alpha(z, 0) = -0.01275(1 - \tanh^2(z - 100)), 50 \leq z < \infty \quad (19)$$

Two Dislocations of Same Sign Between Wells

$$\phi(z, 0) = 0.01275(1 + \tanh z) + 0.012, -\infty < z < 50 \quad (20)$$

$$\phi(z, 0) = 0.01275(1 + \tanh(z - 100)) + 0.0375, 50 \leq z < \infty \quad (21)$$

$$\alpha(z, 0) = 0.01275(1 - \tanh^2(z)), -\infty < z < 50 \quad (22)$$

$$\alpha(z, 0) = 0.01275(1 - \tanh^2(z - 100)), 50 \leq z < \infty \quad (23)$$

## Problem Setup and Constants

The system is observed over the length of the rod. The magnitude of the Burgers vector  $b = 4.05 \times 10^{-10} \text{m}$ , the elastic shear modulus  $c = 2.3 \times 10^{-2} \text{N}\mu\text{m}^2$ , the material constant  $k = \frac{cb^2}{4} = 9.43 \times 10^{-10} \text{N}$ , and  $B = 10^{-16} \text{N-s/B}$ . The energy is at a minimum where  $\bar{\phi} = \pm 0.05$ . Dislocation density  $\alpha$  is expressed in units of  $b^{-1}$ , Time  $t$  is expressed in units of  $\frac{bB}{c}$ , and Velocity  $V$  is expressed in units of  $\frac{c}{B}$ .

## 4 Nondimensionalization

When working with differential equations modeled after real world situations, there are often many different constants and variables within a given equation. Systems can also appear complex and complicated when leaving these constants in the equations, which makes it difficult for looking at certain characteristic properties within the system. When solving more complex problems that involve multiple different units due to the combination of a few or many different variables, having units in the problem can introduce more complexity and can also pose issues to computers when working with such small numbers. A number of benefits could come from converting these equations into a dimensionless form. Specific mathematical techniques become easier to apply to

dimensionless equations, parameters that can be ignored or treated with some approximation could be assigned and thrown away based on the equation, round-off errors could be avoided when working with such small numbers on computer computations, and the solutions can be abstracted to fit other phenomena. By turning an equation full of units and relationships into a simpler problem, the solutions or equations can become physically meaningful to physics, engineering, and mathematical problems.

By nondimensionalizing a problem, all of the independent and dependent variables get substituted for dimensionless quantities that represent that variable. Then working towards simplifying the problem with different techniques allows for a simpler equation, where the features and characteristics of that equations could be better explained.

Starting with the one-dimensional equations that were introduced earlier, it is possible to nondimensionalize these values in order to remove the constants from the equation. This will allow for further analysis of the equations, while removing the units from the equation. Removing these constants will allow the later computation to be more accurate, as the computer does not have to handle too many possible rounding errors when computing the solution.

When nondimensionalizing the one-dimensional equations some terms and variable are redefined into different quantities that are dimensionless. First, the

time and length variables are changed  $t = \tau t_c$ ,  $z = \chi z_c$ , where  $t_c = \frac{bB}{c}$  and

$z_c = b$ . The material constant  $\kappa = \frac{\hat{\kappa}cb^2}{4}$  and the length  $z_c = b$ . When changing

the value of  $\hat{\kappa}$ , a value of zero indicates removing the diffusion term from the system and only having a system of convection, while a value of one would follow the numerical value provided in Acharya[3]. The internal shear stress is forced dimensionless by letting  $\tau = c\hat{\tau}$  and the non-convex energy density becomes

$\eta = c\hat{\eta}$ . The dislocation density becomes dimensionless by letting  $\alpha = \frac{1}{b}\hat{\alpha}$ .

Now, starting with the initial one-dimensional equation for velocity

$$V = -\frac{1}{\tilde{B}}(\mathcal{J} - \eta_\phi + \kappa\partial_z\alpha)\alpha,$$

its non-dimensional version easily obtained by a change of variables, is given by

$$\hat{V} = -\frac{B}{\tilde{B}b}(\hat{\mathcal{J}} - \hat{\eta}_\phi + \frac{\hat{\kappa}}{4}\partial_\chi\hat{\alpha})\hat{\alpha}$$

However, this non-dimensional expression still contains constants that could further be removed when using  $\tilde{B} = B|\alpha| = \frac{B}{b}|\alpha|$ . The non-dimensional expression for velocity becomes:

$$\hat{V} = -(\hat{\mathcal{J}} - \hat{\eta}_\phi + \frac{\hat{\kappa}}{4}\partial_\chi\hat{\alpha})\text{sgn } \alpha$$

Similarly proceeding with the other equations, we obtain the following system:

$$\phi_\tau + \hat{\alpha} \hat{V} = 0 \quad (24)$$

$$\hat{\alpha}_\tau + (\hat{\alpha} \hat{V})_\chi = 0 \quad (25)$$

$$\hat{V} = -(\hat{\mathcal{T}} - \hat{\eta}_\phi + \frac{\hat{\kappa}}{4} \partial_\chi \hat{\alpha}) \operatorname{sgn} \alpha \quad (26)$$

This one-dimensional model considers  $\tilde{B} = B |\alpha|$ , and it is assumed that  $|\alpha| \partial_\chi \hat{\alpha}$  is a weak derivative of  $\frac{1}{2} |\alpha| \alpha$ , so the following equations are obtained:

$$\alpha_\tau - \partial_\chi ((\mathcal{T} - \eta_\phi) |\alpha|) - \frac{1}{4} \partial_\chi (|\alpha| \partial_\chi \alpha) = 0 \quad (27)$$

$$\phi_\tau - \frac{1}{4} \partial_\chi \left( \frac{|\alpha| \alpha}{2} \right) - ((\mathcal{T} - \eta_\phi) |\alpha|) = 0 \quad (28)$$

Again letting  $\mathbf{u} := \begin{pmatrix} \alpha \\ \phi \end{pmatrix}$ , we obtain

$$\mathbf{f}(\mathbf{u}) = \begin{pmatrix} -(\mathcal{T} - \eta_\phi) |\alpha| \\ -\frac{1}{4} \frac{|\alpha| \alpha}{2} \end{pmatrix} \quad (29)$$

$$\mathbf{g}(\mathbf{u}) = \begin{pmatrix} \partial_\chi \left( \frac{1}{4} |\alpha| \partial_\chi \alpha \right) \\ (\mathcal{T} - \eta_\phi) |\alpha| \end{pmatrix} \quad (30)$$

$$D_u(\mathbf{f}) = - \begin{pmatrix} \operatorname{sgn}(\alpha) (\mathcal{T} - \eta_\phi) & \frac{\partial(\mathcal{T} - \eta_\phi)}{\partial \phi} |\alpha| \\ \frac{1}{4} |\alpha| & 0 \end{pmatrix} \quad (31)$$

The eigenvalues become

$$\lambda = \frac{1}{2} \left( \operatorname{sgn}(\alpha) (\mathcal{T} - \eta_\phi) \pm \sqrt{(\mathcal{T} - \eta_\phi)^2 + (\mathcal{T}_\phi - \eta_{\phi\phi}) \alpha^2} \right) \quad (32)$$

## 5 Implementation

For many partial differential equations that were created to explain natural phenomena, solving for an exact solution is difficult and in some cases are not possible. Partial differential equations are also difficult to solve by hand and often require a fair amount of computational power. The solutions to partial differential equations become approximated, as a result, and there are a number of different methods used to find approximate answers for partial differential equations. Various numerical models exist which help solve these mathematical models on computers and only in the simplest cases can a partial differential

equation be solved. In general, solving these equations require a numerical method to obtain an approximate solution.

The Finite Element Method (FEM) serves as a computational method for obtaining a numerical solution of a differential or integral equation. In short, the FEM divides a prescribed object into smaller parts called finite elements with simple behaviors and individually computes each element, combining the results to get an approximate answer in the end. Along with coming up or having an equation, several other requirements are needed to solve the problem. A mesh, or discrete representation of the region, is created that will contain the equation and boundary conditions on this mesh are required in order to link the equation with the region that it is being solved in. The model is initially formulated into some mesh, which gets subdivided into many smaller elements of finite size and finite number of elements. Now the PDE is approximated in each elements, usually with some polynomial that can easily be solved. When solving each element and obtaining approximated solutions, this will yield a matrix. Using a sparse matrix solver (Discontinuous Galerkin Method, Galerkin Method, or Variational approach), the unknown variables in the problem can be solved for.

In order to solve the system of one-dimensional PDEs, the discontinuous Galerkin (DG) method is used to solve for the convective component of the system. The DG methods are within a class of finite element methods that depend on using discontinuous basis functions, normally polynomials, to approximate the system. Next, combining the DG method with the forward Euler method to compute each matrix at each time step. However, since the approximated solution just using this method shows instability near shocks during the computation, the use of a slope limiter allows for further accuracy when computing an approximate solution (Cockburn, 2001). Without a slope limiter, it would often appear as if the velocity reaches some large positive or negative value after awhile leading to unstable solutions. When dividing a defined mesh into a set of finite elements and approximating polynomials onto each element, the slope limiter acts to essentially limit the slope from reaching these large values. Whenever the slope of the plastic deformation graph reaches an arbitrary large value, the slope limiter forces the slope to some smaller value that allows the simulation to continue smoothly.

The software that was used to calculate the system of one-dimensional equations using the finite element method was NGSolve, a multiphysics finite element software. NGSolve allows us to implement physical equations and solution algorithms easily using a rich Python interface to its C++ codebase. With NGSolve, it is possible to define a specific mesh and use a numerical method to visualize the solution or even consider adaptive mesh refinement to get better, more accurate solutions at necessary locations.

## 6 Results and Analysis

A variety of different equilibrium solutions, along with non-equilibrium solutions for the various initial conditions for plastic deformation  $\phi$  are examined in this section.

### No Load:

#### 6.0.1 Single Dislocation

##### Linear Stress

A rod of length  $200b$  is discretized into 5000 elements. A single dislocation is considered at the center of the rod as an initial condition. It was observed that the dislocation does not remain localized as shown in Figure 8, even in the absence of applied strain. The reason for this behavior is the energy description used in this case. Linear elasticity corresponds to a quadratic energy function with a minima at 0 elastic strain. Thus, a dislocation with non-zero plastic distortion or elastic distortion cannot be an equilibrium solution of a system of equations based on linear elasticity. Results of this test case validate this physical result.

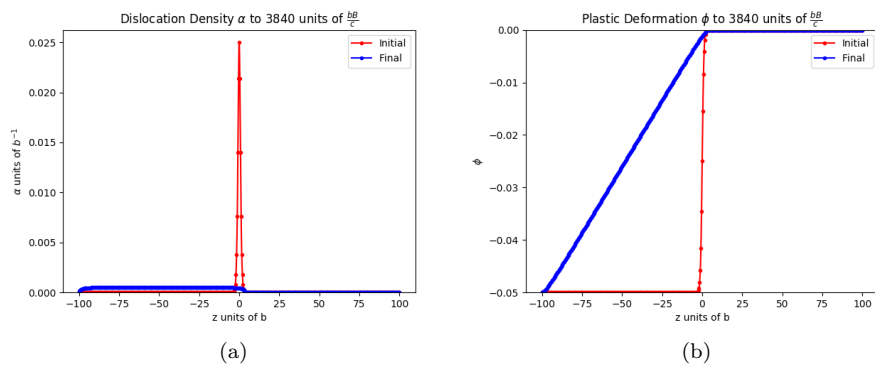


Figure 8: Tanh equilibrium profile with linear stress

### Cubic Stress Connecting Wells

An analytical solution for the initial profile shown in Figure 9 exists for a cubic stress case and is described in Das et al. (2013). Figure 9 illustrates and verifies that the analytical profile matches the result given using the finite element method.

In this case of an equilibrium solution given no load  $g(t) = 0$ , a mesh coarseness of 2000 elements in the mesh is used, along with a rod length of  $100b$  lengths to simulate 20 elements per  $b$  lengths. Polynomials  $p$  of degree 1 are used and approximated onto the mesh and the simulation is ran for  $t = 9667 \frac{bB}{c}$ .

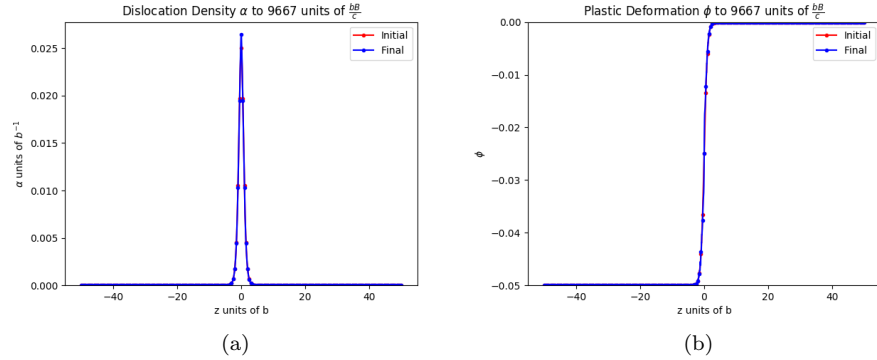


Figure 9: Tanh equilibrium profile with cubic stress

The energy corresponding to a cubic stress has a minima at  $\pm\bar{\phi}$ . Figure 9 appears to have no change, which agrees with the analytical solution since the system is already at a state of minimum energy or equilibrium. Because no load is induced on the system, there should be no change to the system since energy wants to stay at its minimum state rather than forcing dislocations to propagate out of the body of the system.



### Cubic Stress Between Wells

Two cases were done to compare the results with those shown in Das et al (2013): (i) transition layer equidistant from energy wells, and (ii) transition layer non-equidistant from energy wells.

Figure 10 looks at a cubic stress between wells case where the transition layers are equidistant from the energy wells. The simulation is ran through 1111 time steps with a rod length of  $100b$  lengths discretized into 2000 elements.

Figure 11 looks at a cubic stress between wells case where the transition layers are non-equidistant from the energy wells. The simulation is ran through 9667 time steps with a rod length of  $100b$  lengths discretized into 2000 elements.

Results, shown in Figure 10 and 11 are in good agreement with those presented in Das et al. (2013)

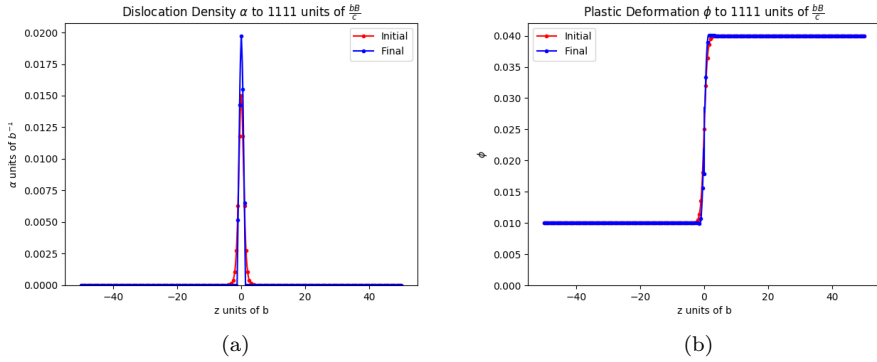


Figure 10: Transition layer equidistant from energy wells

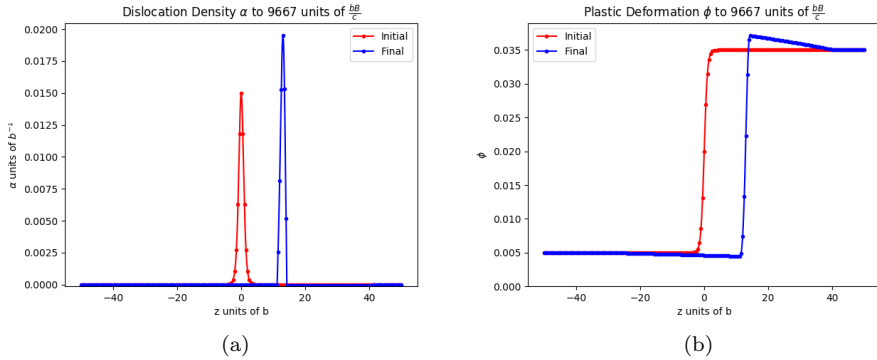


Figure 11: Non-Equilibrium transition layer non-equidistant from energy wells

### 6.0.2 Two Dislocations of Opposite Sign Between Wells

A rod of length  $400b$  is discretized into 8000 elements. Two dislocations of opposite signs are considered in the rod as an initial condition. It was observed that the dislocation remains localized as shown in figure 12 when in the absence of applied strain.

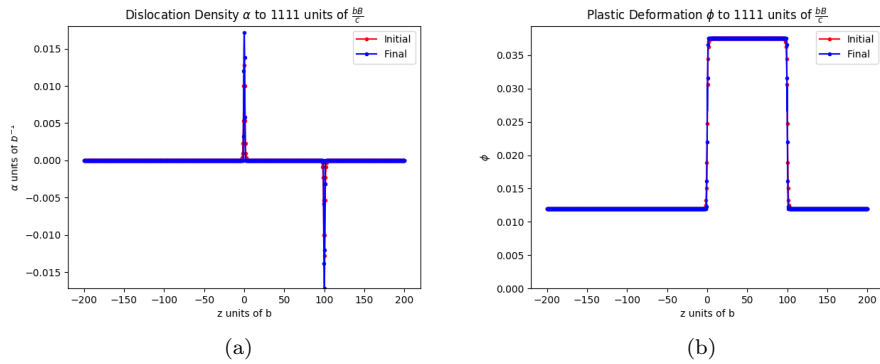


Figure 12: Transition layers between wells corresponding to positive and negative dislocation

Figure 12 shows that when a positive and negative dislocation are adjacent to each other, the form of the  $\phi$  profile remains unchanged.

### 6.0.3 Two Dislocations of Same Sign Between Wells

A rod of length  $400b$  is discretized into 8000 elements. Two dislocations of the same sign are considered in the rod as an initial condition. It was observed that the dislocation changes structure as shown in figure 13 when in the absence of applied strain. Since the system is in non-equilibrium, the tendency to reach equilibrium induces change when subject to no load.

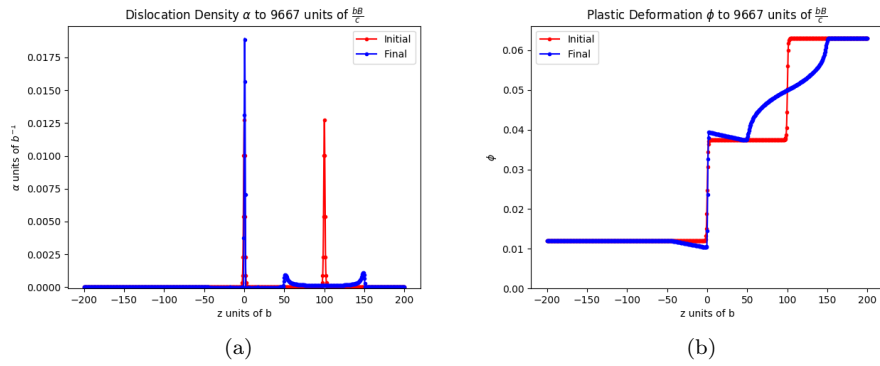


Figure 13: Non-Equilibrium transition layers between wells corresponding to only positive dislocations

### 6.0.4 Multiple Dislocations Connecting Wells

A rod of length  $400b$  is discretized into 8000 elements. Multiple dislocations corresponding to both positive and negative dislocations are considered in the rod as an initial condition. In the absence of applied stain, figure 14 stays unchanged due to the state of equilibrium. Whether or not the dislocations

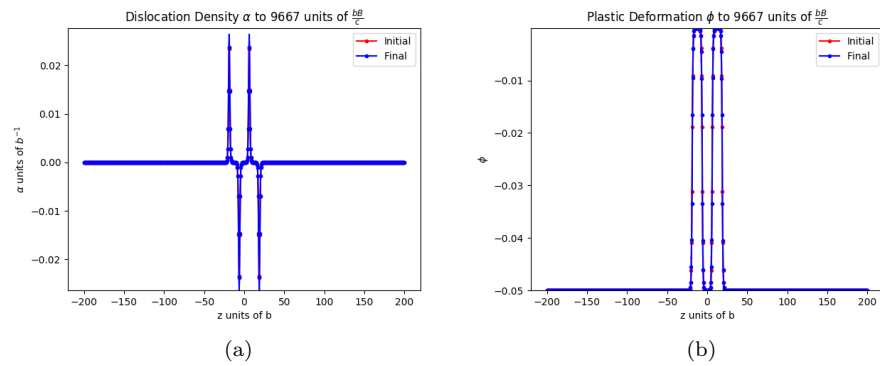


Figure 14: Two equilibrium transition layers connecting wells corresponding to positive and negative dislocations

are of the same or opposite signs with one another, the corresponding  $\phi$  profile stays in quasi-equilibrium due to the ends of the profile being connected to the energy wells. The system remains in equilibrium and at the lowest energy state without applying load.

## Applying Load:

### 6.0.5 Single Dislocation

#### Cubic Stress Connecting Wells

A physical problem of a single dislocation moving under the application of stress is modeled in this section. Cubic stress case is considered.

In this case of an equilibrium solution given many different loads  $g(t)$  ranging from  $g(t) = 0$  to  $g(t) = 0.025$  shows a range of different solutions after running the simulation for 7500 time steps. As figure 14a shows, using greater loads will force dislocations to propagate out of the body while showing signs of both convection and diffusion.

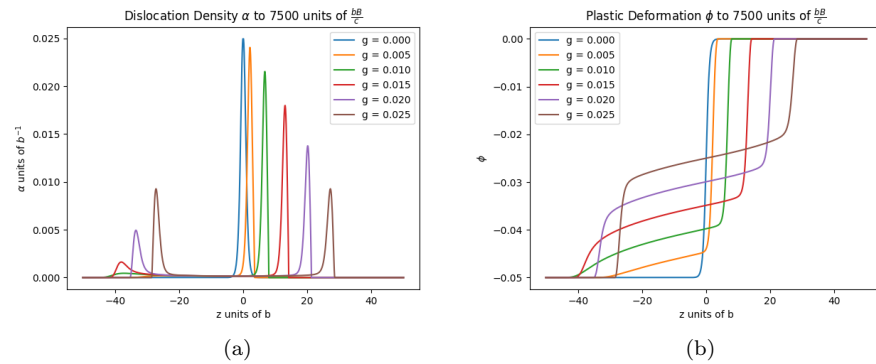


Figure 15: Tanh equilibrium profile

Applying different values of load induce different properties in the shape and motions of dislocations. The dislocation's shape may change with load, however, the entire system still appears to remain as a localized entity that propagates towards the boundary of the system.

### 6.0.6 Two Dislocations of Opposite Sign Between Wells

When applying load to two dislocations of opposite sign in between wells, the natural nature would be to reach a state of minimum energy as quickly as possible. Given an applied load of  $g(t) = 0.005$ , a rod length of  $300b$  lengths, and ran through 7500 time steps. In this case, a mesh coarseness of 6000 elements within the mesh is used, which gives 20 elements per  $b$  length.

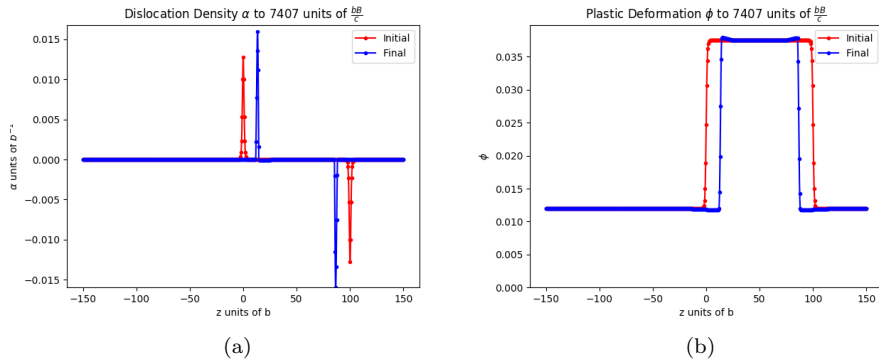


Figure 16: Transition layers between wells corresponding to positive and negative dislocations

As seen in figure 16(a), the two dislocations are initially in a state of non-equilibrium after applying load. As a result, the two dislocations attract one another and move towards each other. Eventually, the dislocations will propagate towards each other until they simulate destructive interference when they meet up, which will cancel out the dislocations. The two dislocations propagate towards each other since that is the shortest path towards reaching a state of minimum energy and equilibrium.

## 7 Conclusion/Future Plans

The results produced by the finite element method confirm the results found using finite difference methods (Das et al, 2013). The finite element method allows the modeling of one-dimensional dislocations through no load and with load, however, takes more computational power to simulate the same results. The finite difference method produces the same results more rapidly, however, extending this approach to three dimensions involves introducing slip layers corresponding to certain specified slip planes. On the other hand, extending from a one-dimensional model of dislocations to three-dimensions using an advanced discontinuous Galerkin method would not involve introducing slip layers. As a result, using different numerical schemes to solve a one-dimensional field dislocation mechanics model seems applicable in this scenario.

It is possible to generate a crystalline object and simulate the behavior of dislocations through stresses. The FDM model allows for the prediction of the propagation of dislocations through a material. The FDM model overcomes the issues presented by the macroscopic elastoplastic models, while also considering the reliability of atomistic models. By using the discontinuous galerkin method, it was possible to obtain results through simulations that modeled the microscopic scale phenomenon involving one or a few dislocations.

For initial conditions within connecting energy wells, applying no load indicates that the system already exists in a state of minimum energy, so dislocations would just appear to stay unchanged within the atomic structure of the material. However, in cases where the crystalline structure is in a state of non-equilibrium with no applied load, the dislocations would still attempt to propagate out of the material since energy systems tend to gravitate towards the lowest energy levels. When applying load to these dislocations, these systems are removed from their state of equilibrium. As a result, the dislocations attempt to propagate out of the material or towards other dislocations in order to reach a state of minimum energy.

Since different numerical schemes involving the field dislocation mechanics model have succeeded in producing similar results, it would be possible to extend these approaches to three-dimensions. In the future, the advanced discontinuous Galerkin method could be implemented to the existing model to model dislocations in three-dimensions. After understanding the nucleations and evolutions of dislocations, it would be possible to predict plastic deformation mechanisms in crystalline materials. Understanding these crystalline materials allow for designing superior materials that could sustain different conditions. Through the use of theoretical and computational frameworks, it may be possible in the future to model dislocations for micron-sized crystalline components and predict their behavior with other defects quantitatively. Understanding and being able to predict and model dislocations in crystalline materials would allow for better implementation in technology or related fields.

## 8 Acknowledgements

I would like to express my gratitude towards my team that have provided support throughout this research project. I would like to acknowledge Christof Teuscher and Jay Gopalakrishnan for giving me the opportunity to take part in an undergraduate research program and letting me explore the research field given a project along with concepts that were a complete mystery to me beforehand. A special thanks goes to my student mentor and teammate, Dow Drake, who taught and informed me about everything I needed to know about the math side of dislocations and plastic deformation. Dow worked with me daily in order to provide me with the knowledge and support necessary to carry out this research paper, as well as, providing me with the code and tools necessary to simulate dislocations through the use of computational tools. Many thanks goes to the city partner, Saurabh Puri, for informing me on the physics and engineering side of plastic deformation and dislocations and working towards helping the team achieve an end goal. Also, I am grateful to Tathagata Goswami for taking his time to teach me and guide me through solving partial differential equations with the finite element method, as well as, helping me understand the tools used in NGSolve.

The REU Site is supported by the National Science Foundation under grant no 1758006.



## 9 References

Acharya, A., 2001, A model of crystal plasticity based on the theory of continuously distributed dislocations, *Journal of the Mechanics and Physics of Solids* 49, 761- 785.

Acharya, A., 2003, Driving forces and boundary conditions in continuum dislocation mechanics, *Proceedings of the Royal Society A* 459, 1343- 1363.

Amit Das, Amit Acharya, Johannes Zimmer, and Karsten Matthies. Can equations of equilibrium predict all physical equilibria? a case study from field dislocation mechanics. *Mathematics and Mechanics of Solids*, 18(8):803–822, 2013.

Amit Acharya. New inroads in an old subject: plasticity, from around the atomic to the macroscopic scale. *Journal of the Mechanics and Physics of Solids*, 58(5):766–778, 2010.

Bernardo Cockburn, and Chi-Wang Shu. Runge-Kutta Discontinuous Galerkin Methods for Convection-Dominated Problems. *Journal of Scientific Computing*, Vol. 16, No.3, 2001.

Dimiduk DM, Woodward C, LeSar R, Uchic MD (2006) Scale-free intermittent flow in crystal plasticity. *Science* 312:1188–1190.

Uchic, M.D.; Dimiduk, D.M.; Florando, J.N.; Nix, W.D. Sample dimensions influence strength and crystal plasticity. *Science* 2004, 305, 986–989.

William D. Callister Jr., *Fundamentals of Materials Science and Engineering*, 2001.

Xiaohan Zhang, Amit Acharya, Noel J. Walkington, Jacobo Bielak. A single theory for some quasi-static, supersonic, atomic, and tectonic scale applications of dislocations. *Journal of the Mechanics and Physics of Solids*, Vol. 84, pp. 145-195, 2015.